Developing Low-Cost, Simplified, and Open-Source Durafet-based pH Instrument Electronics

Amelia L. Ritger
Ecology, Evolution, and Marine Biology
University of California, Santa Barbara
Santa Babara, USA
aritger@ucsb.edu

David C. Burnett
Electrical and Computer Engineering
Portland State University
Portland, USA
dburnett@ece.pdx.edu

OCEANS 2023 - Limerick | 979-8-3503-3226-1/23/$31.00 ©2023 IEEE | DOI: 10.1109/OCEANSLimerick52467.2023.10244512

***Abstract*— Ocean acidification monitoring efforts are a crucial component of tracking the impacts of climate change in marine ecosystems. However, the high instrument cost presents a major barrier to the production of scientific knowledge and has resulted in a highly fragmented understanding of the global progression of acidification. Our project built upon an existing nearshore marine pH sensor design which utilizes a Durafet pH electrode. Our goal was to lower barriers to access by significantly lowering the cost of, and improving approachability to, the design and use of pH sensor electronics. We have created a more compact design using open-source components based on the popular and easy-to-use Arduino platform that eliminates over $900 from the cost of the sensor electronics. We demonstrate with lab and field testing that switching to Arduino-based sensor electronics maintains high data fidelity. Our design supports open science by allowing more individuals and research groups to engage in high-quality oceanographic research.**

Keywords*— *Instruments, marine, monitoring, oceanography

I. Introduction

Ocean acidification occurs when seawater pH declines as a result of the ocean absorbing anthropogenically produced carbon dioxide from the atmosphere. Acidification is an increasingly prevalent environmental stressor with measurable effects on marine ecosystems, including disrupting trophic interactions [1] and reducing calcification rates of ecologically and economically important marine species [2].

Unfortunately, near-shore oceanographic monitoring efforts largely rely upon commercially available sensors that are bulky and expensive. These monitoring programs often require large research budgets to cover the initial equipment purchase, as well as sustained funding to pay for annual maintenance and calibration fees. This presents a major barrier to comprehensive environmental monitoring, as financial support for long-term monitoring programs is limited [3] and well-funded research groups are more likely to receive additional funding [4], [5]. With limited research groups able to access the funding to start and maintain their own oceanographic monitoring programs, there are consequently few pH sensors deployed in the nearshore marine environment. This patchy network of sensors contributes to the current uncertainty on the progression of ocean acidification in many ecosystems – especially in regions that have been deemed particularly vulnerable to acidification [6].

Oceanographic research presents an opportunity for improved accessibility and thus better science with the development of lower cost instrumentation. Low-cost, open-source instrumentation is becoming an increasingly popular method for environmental sensing in a variety of systems [7]–[9]. In the marine environment, for example, the Cave Pearl Project and Oceanography for Everyone have both used open-source, Arduino-based systems to create inexpensive alternatives to commercially available environmental monitoring sensors [10], [11]. The adoption of these methods increases access to environmental monitoring technologies and subsequently expands the spatial and temporal coverage of environmental data [12]. Ocean acidification monitoring programs would benefit from lower cost instrumentation, as more deployed sensors would facilitate more comprehensive measurements characterizing pH variability across time and space. Increasing access to oceanographic monitoring will support scientific research to assess the state of our oceans and predict how future climate scenarios may threaten marine ecosystems.

Our project sought to improve upon a current pH sensor design which utilizes a commercially available Honeywell Durafet Ion Sensitive Field Effect Transistor (ISFET) pH electrode [13] and is widely used to collect autonomous intertidal pH measurements [14]–[20]. We used off the shelf components and an Arduino-based data logger to create an open-source design that may be built by anyone with access to basic electronics equipment. We demonstrate that our new data logger collects seawater pH and temperature measurements comparable to the old design, at a fraction of the cost.

II. Methods

A. Design

Our goal was to design an open source data logger that would read the electrical signals from the Durafet pH electrode and generate an output comparable to the old data logger design, at a significantly lower cost and complexity by using an Arduino-based microcontroller. Our design was motivated by the following requirements:

- Built using low-cost, readily available components
- Operating life span similar to the old data logger design (at least 6 months)
- Compact footprint to fit neatly in sensor housing

- Interfacing with non-proprietary software and standard USB connectors
- User-adjustable deployment parameters, such as start time and sampling interval
- Removable microSD storage

The old sensor design uses the commercially available VoltX data logger (including a 24-bit ADC) manufactured by MadgeTech [21], paired with a custom-manufactured voltage divider (original design by [22]; Fig. 1). MadgeTech offers free, proprietary software to communicate with the VoltX data logger in order to configure the logger and download data through a standard USB-A to Micro USB interface cable. The old design requires one 9 V LiON battery to power the data logger and two 3.6 V LiON batteries to power the Durafet pH electrode.

In our new design, we used an Adafruit Feather M0 Adalogger (including a 10-bit ADC, not used for sensor digitization) [23] paired with an Adafruit DS3231 Precision real-time clock (RTC) [24], an Adafruit ADS1015 12-bit ADC [25], an Adafruit ADS1115 16-bit ADC [26], and off the shelf passive components (Fig. 1). Communication with the Arduino occurs through the free Arduino IDE via a USB-A to Micro USB cable. The new design eliminates the 9 V LiON battery and only requires two 3.6 V LiON batteries to power all sensor electronics.

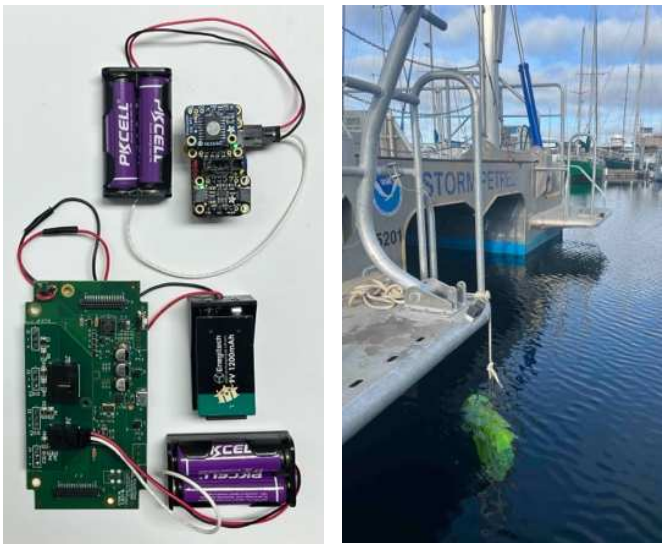

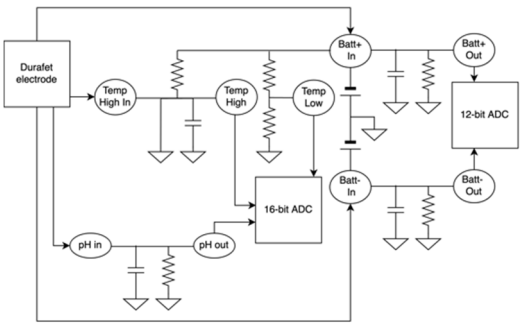

Fig. 1. *Top left*: Side-by-side comparison of old (MadgeTech, bottom) and new (open-source, top) sensor electronics. *Top right*: Packaged sensor systems concurrently deployed in a dive bag for field deployments in Port Angeles Harbor, Washington. *Bottom*: Circuit schematic of the voltage divider circuits joining the pH electrode to the ADC inputs [22].

The Adalogger's single-ended 10-bit ADC only provides 1024 sampling levels, and so we added Adafruit 12-bit and 16-bit ADCs to increase sampling resolution and allow for the differential signals needed to sample negative voltages. Both ADCs have programmable gain amplifiers, and so we further increased sampling resolution by increasing the gain to 8x on the 12-bit ADC (1 least significant bit = 250 μV) and to 4x on the 16-bit ADC (1 least significant bit = 31.25 μV).

Additionally, the Adalogger's on-board crystal oscillator exhibits temperature-dependent drift and requires external input to accurately log date and time, and so we used the Adafruit precision RTC in our design. The precision RTC has a temperature-compensated crystal with ±2 minutes drift per year [24], making it more suitable for environmental monitoring applications with long unattended deployment times.

The materials cost for both designs is presented in Table 1. Documentation and instructions for building the new design are available on GitHub under the Apache 2.0 license: `https://github.com/ameliaritger/arduino-ph-sensor`.

B. Testing

We compared performance of the new design with the old design using two Honeywell Durafet II pH electrodes [27] connected to each data logger design via a Honeywell Cap Adapter [28].

In order to fairly compare performance of the new and old data logger designs, we needed to account for the known sensor-to-sensor offset in each Durafet electrode. We achieved this in the lab by using two Durafets, each connected to a data logger of either the new or old design, and repeating the measurements with the electrode originally connected to the other data logger. For these "sensor swaps", we placed sensors in equimolar tris in artificial seawater (hereafter, "tris"), a buffer with a pH that is well defined as a function of temperature [29], [30], to draw comparisons between designs in a solution with a known pH. Sensors were directly next to each other in the same tris solution in a 25 ºC water bath and collected readings every 15 seconds for a total of 2 hours. After 1 hour, we swapped the data loggers between pH electrodes to isolate sensor effects from data logger effects on pH and temperature measurements. We performed sensor swaps with the new design and old design data loggers, in addition to two data loggers of the old design, to isolate

TABLE I. COST COMPARISON BETWEEN THE SENSOR ELECTRONICS OF THE OLD DESIGN, WHICH USES COMMERCIALLY AVAILABLE AND CUSTOM MANUFACTURED COMPONENTS, AND THE NEW DESIGN, WHICH USES COMMERCIALLY AVAILABLE AND OFF THE SHELF COMPONENTS. COMPONENT MANUFACTURERS ARE LISTED IN PARENTHESES.

Item	Old design	New design
Data logger[a]	$649 (MadgeTech)	$67 (Adafruit)
Voltage divider PCB	$400 (Go Tech Corp)	$22 (Adafruit)
Batteries	$14	$9
Total cost[b]	**$1063**	**$98**

[a.] Electronics required to digitize Durafet analog voltages and store them in local nonvolatile memory
[b.] Excludes fixed costs (e.g., the Durafet and PVC housing) which are the same for both designs

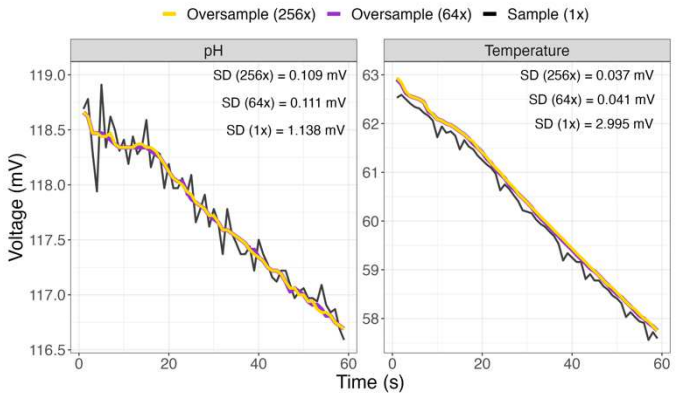

Fig. 2. Oversampling rate comparison between 256x (yellow) and 64x (purple) oversampled data, and 1x (black) sampled data for pH (left) and temperature (right) pins on the new design data logger. Standard deviations (SD) are displayed for each sampling rate. Each time point represents a 10 second sampling period for a total of 10 minutes.

differences between sensors and data loggers. To reduce noise and achieve a similar resolution to the old data logger, the new data logger oversampled the temperature and pH signal 256 times (Fig. 2).

We also evaluated performance of our new design in a real-world scenario using field deployments to monitor measurement differences between designs *in situ*. Sensors were configured with either a new design or old design data logger and deployed in the Port Angeles Harbor (Washington, U.S.) on December 15, 2022, for 24 hours (Fig. 1). We placed sensors immediately next to each other in a dive bag that was sunk to approx. 1 meter depth in the harbor. Sensors collected readings every 5 minutes. To reduce noise and achieve a similar resolution to the old data logger, the new data logger oversampled the temperature and pH signal 64 times. We reduced the oversampling rate for field deployments as a conservative measure to preserve battery life, because field deployments occurred prior to collecting measurements on current consumption between oversampling rates.

Finally, we measured current consumption for each data logger design using a voltage drop over a 1 Ω shunt resistor in series with each data logger's battery power supply [31], [32]. Voltage and current measurements were collected on a Keithley DMM6500 multimeter [33] and Rigol DS1054Z oscilloscope [34]. We measured the current draw from each design while sampling and idle, in addition to current draw from the new design at oversampling rates of 64x and 256x.

C. Analysis

We temperature calibrated sensors using known temperature readings measured by an Onset HOBO Tidbit water temperature data logger [35] in an ice bath, at stable room temperature, and in a 25 ºC water bath. We calibrated temperature readings for each sensor by fitting a line to the mean temperature measured by the HOBO logger and the difference in temperature readings between each pH sensor and the HOBO logger. We then tris calibrated sensors using tris buffer at stable room temperature (20.3 ± 0.2 ºC) and applied calibration values to each unique Durafet-logger pairing.

To analyze sensor swap data, we calculated the theoretical difference between data loggers by subtracting the mean differences in temperature and pH voltage readings between data loggers before and after the sensor swap, which allowed us to account for differences attributed to individual pH electrodes. We then converted voltages to temperature and pH units and determined differences between data loggers by subtracting the mean temperature and pH readings before and after the sensor swap, and then averaging those values between time periods. We converted voltages to pH and temperature values using equations found in [13].

All data were analyzed and visualized using R version 4.1.1.

III. Results

A. Sensor swap

The average difference in temperature voltage readings between new and old design sensors before and after the swap was 1.7 and 1.4 mV, respectively. The average difference in pH voltage readings between sensors before and after the swap was 32.1 and 32.0 mV, respectively. We therefore estimate the average difference between the new and old design data loggers, after accounting for pH electrode variation, was between 0.2 and 0.3 mV (Fig. 3), which corresponds to an approx. difference of 0.5 ºC and 0.002 pH units. In comparison, the old design data loggers measured temperature voltage readings with average differences of 0.05 and 0.12 mV before and after the swap, respectively. The average difference in pH voltage measurements before and after the swap were 31.6 and 32.3 mV,

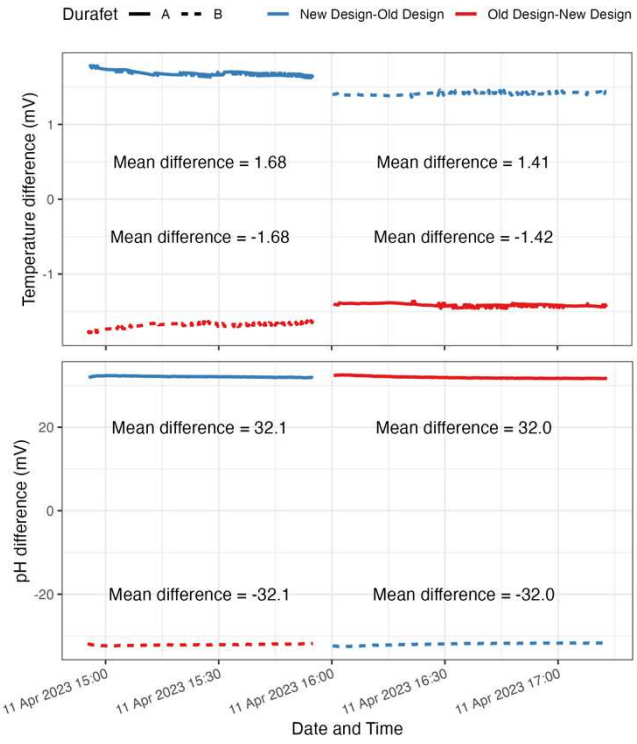

Fig. 3. Differences in temperature (top) and pH (bottom) voltage measurements collected by the new (blue) and old (red) data logger designs sensor swaps in a 25 ºC water bath. Voltage measurements do not exclude differences attributed to individual Durafet electrodes.

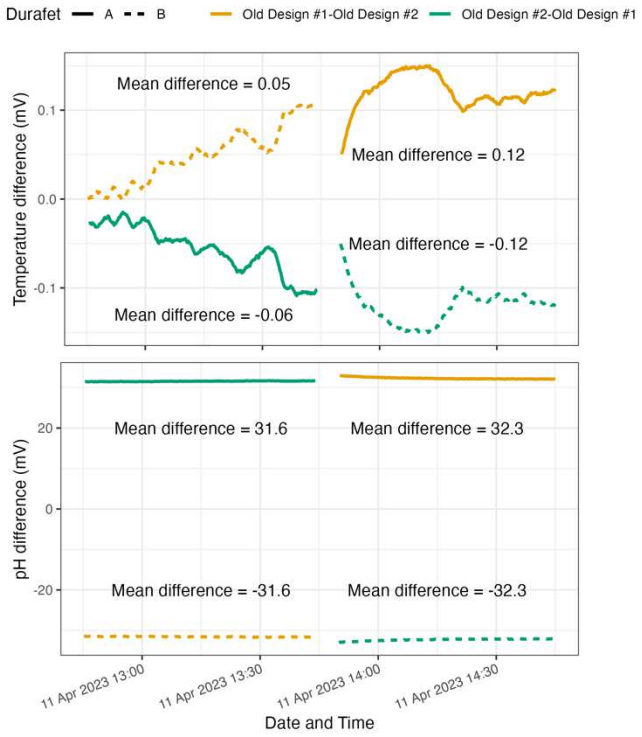

Fig. 4. Differences in temperature (top) and pH (bottom) voltage measurements collected by two old design (#1: orange; #2: green) data loggers during sensor swaps in a 25 ºC water bath. Voltage measurements do not exclude differences attributed to individual Durafet electrodes.

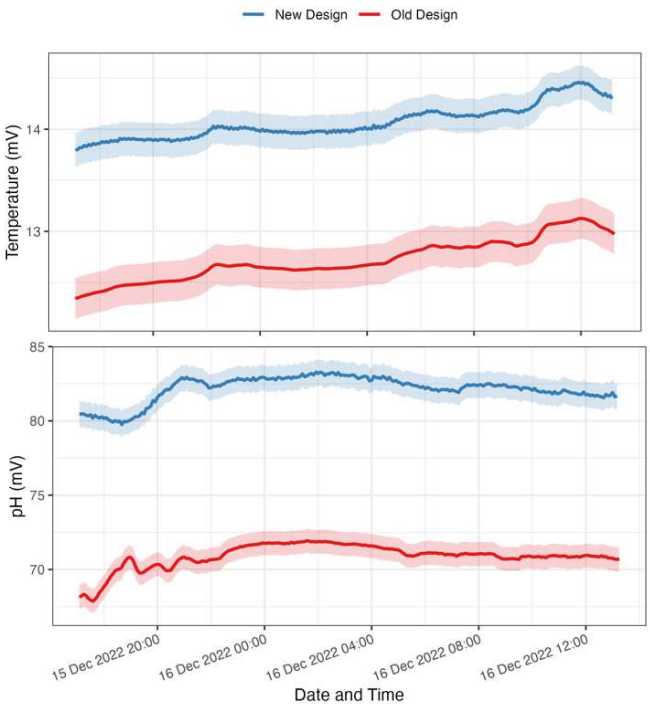

Fig. 5. Temperature (top) and pH (bottom) voltage measurements collected by the new (blue) and old (red) design data loggers during the field deployment in December 2022. Shaded areas represent the standard deviation for each design. Voltage measurements do not exclude differences attributed to individual Durafet electrodes.

respectively. We therefore estimate the old design data loggers measure average differences between 0.1 and 0.7 mV (Fig. 4), which corresponds to an approx. difference of 0.4 ºC and 0.01 pH units.

B. *Field deployment*

During the field deployment, both data loggers measured similar trends in temperature and pH voltage readings after the first 6 hours, with voltage offsets of sizes expected from sensor-to-sensor variability (Fig. 5). The range of temperature voltage measurements was 0.7 mV for the new design and 0.8 mV for the old design, and the range of pH voltage measurements was 3.5 mV for the new design and 4.1 mV for the old design. The standard deviation of temperature measurements was ±0.2 mV for both the new and old design, and the standard deviation of pH measurements was ±0.9 mV for the new design and ±0.8 mV for the old design. These differences in standard deviation between designs correspond to an approximate difference of 0.02 ºC and $7x10^{-4}$ pH units.

C. *Power consumption*

While sampling, the old design has an average current draw of approx. 2 mA and a maximum current draw of approx. 90 mA over 1 second. The new design has an average current draw of approx. 12 mA and a maximum current draw of approx. 30 mA while sampling, which takes 2 seconds when using a 64x oversampling rate. When not sampling, the old design draws approx. 1 mA current, whereas the new design has an approx. 2 mA current draw (Fig. 6). Oversampling at 256x increases the sampling time to 8 seconds; therefore, with the current configuration at a sampling rate of 1 sample every 10 minutes, oversampling at 256x consumes 5% more power than at 64x.

IV. Discussion

This project's aim was to improve the design of a current pH sensor by lowering costs and making sensor electronics accessible to a wider audience while maintaining a high level of measurement accuracy. The measured differences between sensors were significantly higher than the estimated difference between data loggers, and the measurements collected by the new design were comparable to the old design during sensor swaps. Therefore, we conclude the proposed electronics have a negligible effect on data fidelity. Our findings demonstrate that our design, which uses equivalent sensor electronics that cost $965 less than the original design, is an effective and lower-cost alternative to measuring seawater pH and temperature.

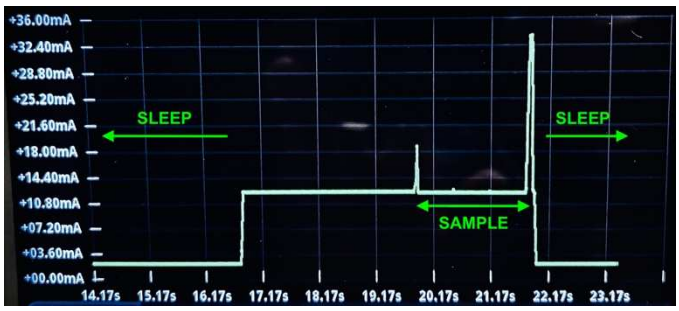

Fig. 6. Current readings from the new data logger design during sleep mode (approx. 2 mA) and while sampling (approx. 12mA).

Our design uses a more streamlined and customizable Arduino-based data logger to meet most of the identified project goals and requirements. Users with access to basic electronics equipment are able to use our design to build their own low-cost data logger with off the shelf components, program their own deployment parameters, and download data without proprietary software. Our design not only reduces the upfront cost of data logger electronics, but it also lowers the cost of regular equipment maintenance and response to catastrophic events such as flooding of the sensor housing by using a modular design with inexpensive, easily-replaceable components.

The measured differences in pH and temperature readings between data logger designs were significantly lower than the measured differences between pH electrodes, even after calibration. Differences between the old and new designs are likely not due to the Adafruit ADCs, as the offset voltages for both the 12-bit and 16-bit ADC at 3.3 V are approx. -100 μV [25], [26], which is significantly lower than the observed voltage differences. Internal sensor differences, however, are a well-acknowledged phenomenon with autonomous sensors [36], [37], and sensor differences can be corrected with independent validation and adjustment to achieve climate quality data [38].

However, in a temperature-controlled water bath during sensor swaps, we observed two old design data loggers collected temperature and pH readings that were different by 0.4 ºC and 0.012 pH units, whereas the differences between the new design and the old design were only 0.5 ºC and 0.002 pH units. Through our testing and analysis, we observed degradation of one Durafet, and we suspect the poor performance of the old design data loggers was due to sensor failure, rather than data logger differences. After excluding the degrading sensor data from analyses, the differences in temperature and pH readings between the new design and the old design were 0.3 ºC and 0.002 pH units, and the differences between the two old design data loggers were 0.3 ºC and 0.001 pH units. Both of these pH differences are well within the standard uncertainties proposed by the Global Ocean Acidification Observing Network [38].

A. Considerations

The new design is a considerable improvement over the old design, given the significant reduction in cost without a significant effect on data fidelity. Nevertheless, the new design has room for even more improvements and further optimization with regards to power consumption. The old design does not allow users to optimize power consumption, and has periods of high current draw while not sampling (presumably, waking up to check for the sampling time). In contrast, our design can be programmed to sleep until the sampling time, which can maximize power savings.

However, our design currently has significantly higher power consumption than the old design, due to the elevated current draw while in idle mode. The current sleep configuration only lowers the current draw to 2 mA, although there is evidence that microcontroller sleep modes may achieve current consumptions as low as 1 μA [39]. As most of the power consumption occurs while the device is in sleep mode (e.g., during sampling intervals of 10 to 30 minutes during field deployments), reducing the current draw an order of magnitude would vastly improve and outperform the lifespan of the old design. With the current power consumption and sampling configuration, the new design's two 3.6V LiON batteries each have a capacity of 2400 mAh and therefore we expect an overall system lifetime of 49 days before the battery that powers the data logger needs to be changed or recharged.

Our decision to use a removable microSD card, in order to increase ease of use for data storage and retrieval, may be one main source of the elevated power consumption while in idle mode. The use of a microSD card increases power requirements during card initialization and operations [40], which likely corresponds to the high current draw events we observed during sampling (Fig. 6). Moreover, microSD cards may be a source of current leakage between sampling intervals, increasing current draw while the microcontroller is in idle mode by an order of magnitude [41]. However, there is evidence that slight hardware and software modifications may circumvent this and other sources of power loss [10].

B. Recommendations

Oversampling with the new design enhances the resolution of data to more closely match the 24-bit ADC of the current design. For our tests, we used both 64x and 256x oversampling rates. Although both oversampling rates allowed us to achieve pH errors well below climate quality thresholds [38] and oversampling at 256x had a negligible overall power consumption increase, the reduced measurement variation at 256x only has a minor effect on temperature and pH measurements (approx. $2x10^{-3}$ and $3x10^{-5}$, respectively; Fig. 6).

Additionally, our new design uses off the shelf passive components with higher tolerances than the surface mount components of the old design. To achieve temperature and pH uncertainties equivalent to the original design and reinforce comparability across designs, we recommend using components with equivalent (1%) tolerances. It is also possible to account for variability in component values during data processing by applying real resistor values to conversion equations [13]. Although passive component values are only directly applied to the temperature calculation, calculations of pH are affected by temperature and consequently pH is indirectly also affected by the resistor values. Therefore, we recommend measuring resistor values before soldering components to ensure accurate calculations of pH and temperature from measured voltages for each sensor.

V. Conclusion

We have demonstrated a field-deployable temperature and pH sensor system that can collect data with high accuracy using off the shelf components that are open-source, reconfigurable, and less expensive than the current state-of-the-art. Using an Arduino-based data logger reduces the prohibitive cost barrier to oceanographic research and enables individuals and groups with modest research budgets to monitor ocean pH conditions. Increasing the number of researchers able to access oceanographic equipment supports more comprehensive tracking of ocean acidification and other climate stressors in the marine environment.

ACKNOWLEDGMENTS

This work would not have been possible without inspiration and support from A. Baish. We would like to graciously thank F. Chan for his expertise and guidance on the original design of the pH sensor and B. Roberts for his time and support collecting power measurements on the oscilloscope. We would also like to thank A. Thompson for her generosity with sharing laboratory glassware. This material is based upon work supported by the National Science Foundation Graduate Research Fellowship Program under Grant No. 2139319. Any opinions, findings, and conclusions or recommendations expressed in this material are those of the author and do not necessarily reflect the views of the National Science Foundation.

REFERENCES

[1] B. M. Jellison and B. Gaylord, "Shifts in seawater chemistry disrupt trophic links within a simple shoreline food web," *Oecologia*, vol. 190, no. 4, pp. 955–967, 2019, doi: 10.1007/s00442-019-04459-0.

[2] L. Mekkes *et al.*, "Pteropods make thinner shells in the upwelling region of the California Current Ecosystem," *Sci. Rep.*, vol. 11, no. 1731, pp. 1–11, 2021, doi: 10.1038/s41598-021-81131-9.

[3] D. B. Lindenmayer and G. E. Likens, *Effective ecological monitoring*, Second Ed. Clayton South, Vic.: CSIRO Publishing, 2018.

[4] B. A. Jacob and L. Lefgren, "The impact of research grant funding on scientific productivity," *J. Public Econ.*, vol. 95, no. 9–10, pp. 1168–1177, 2011, doi: 10.1016/j.jpubeco.2011.05.005.

[5] S. Wessely, "Peer review of grant applications: what do we know?," *Lancet*, vol. 352, no. 9124, pp. 301–305, Jul. 1998, doi: 10.1016/S0140-6736(97)11129-1.

[6] K. Grant, "Exploring Options for an Olympic Coast Ocean Acidification Sentinel Site (OASeS)," 2018. [Online]. Available: https://policycommons.net/artifacts/1769310/exploring-options-for-an-olympic-coast-ocean-acidification-sentinel-site-oases/2500956/.

[7] J. G. Mickley, T. E. Moore, C. D. Schlichting, A. DeRobertis, E. N. Pfisterer, and R. Bagchi, "Measuring microenvironments for global change: DIY environmental microcontroller units (EMUs)," *Methods Ecol. Evol.*, vol. 10, no. 4, pp. 578–584, 2019, doi: 10.1111/2041-210X.13128.

[8] P. Kumar *et al.*, "The rise of low-cost sensing for managing air pollution in cities," *Environ. Int.*, vol. 75, pp. 199–205, 2015, doi: 10.1016/j.envint.2014.11.019.

[9] K. Chan *et al.*, "Low-cost electronic sensors for environmental research: Pitfalls and opportunities," *Prog. Phys. Geogr.*, vol. 45, no. 3, pp. 305–338, 2021, doi: 10.1177/0309133320956567.

[10] P. A. Beddows and E. K. Mallon, "Cave pearl data logger: A flexible arduino-based logging platform for long-term monitoring in harsh environments," *Sensors (Switzerland)*, vol. 18, no. 2, 2018, doi: 10.3390/s18020530.

[11] A. Thaler, K. Sturdivant, R. Neches, and I. Black, "OpenCTD Construction and Operation," 2020. [Online]. Available: https://github.com/OceanographyforEveryone/OpenCTD.

[12] J. S. Horsburgh, J. Caraballo, M. Ramírez, A. K. Aufdenkampe, D. B. Arscott, and S. G. Damiano, "Low-cost, open-source, and low-power: But what to do with the data?," *Front. Earth Sci.*, vol. 7, no. April, pp. 1–14, 2019, doi: 10.3389/feart.2019.00067.

[13] T. R. Martz, J. G. Connery, and K. S. Johnson, "Testing the Honeywell Durafet® for seawater pH applications," *Limnol. Oceanogr. Methods*, vol. 8, no. MAY, pp. 172–184, 2010, doi: 10.4319/lom.2010.8.172.

[14] M. H. Pespeni, F. Chan, B. A. Menge, and S. R. Palumbi, "Signs of adaptation to local pH conditions across an environmental mosaic in the california current ecosystem," *Integr. Comp. Biol.*, vol. 53, no. 5, pp. 857–870, 2013, doi: 10.1093/icb/ict094.

[15] F. Chan *et al.*, "Persistent spatial structuring of coastal ocean acidification in the California Current System," *Sci. Rep.*, vol. 7, no. 1, pp. 1–7, 2017, doi: 10.1038/s41598-017-02777-y.

[16] K. J. Kroeker *et al.*, "Interacting environmental mosaics drive geographic variation in mussel performance and predation vulnerability," *Ecol. Lett.*, vol. 19, no. 7, pp. 771–779, 2016, doi: 10.1111/ele.12613.

[17] G. E. Hofmann, T. G. Evans, M. W. Kelly, C. A. Blanchette, L. Washburn, and F. Chan, "Exploring local adaptation and the ocean acidification seascape – studies in the California Current Large Marine Ecosystem," pp. 1053–1064, 2014, doi: 10.5194/bg-11-1053-2014.

[18] N. V. C. Ralston, C. R. Ralston, J. L. Blackwell, and L. J. Raymond, "Dietary and tissue selenium in relation to methylmercury toxicity," *Neurotoxicology*, vol. 29, no. 5, pp. 802–811, 2008, doi: 10.1016/j.neuro.2008.07.007.

[19] T. G. Evans, F. Chan, B. A. Menge, and G. E. Hofmann, "Transcriptomic responses to ocean acidification in larval sea urchins from a naturally variable pH environment," *Mol. Ecol.*, vol. 22, no. 6, pp. 1609–1625, 2013, doi: 10.1111/mec.12188.

[20] J. M. Rose *et al.*, "Biogeography of ocean acidification : Differential field performance of transplanted mussels to upwelling-driven variation in carbonate chemistry," pp. 1–25, 2020, doi: 10.1371/journal.pone.0234075.

[21] MadgeTech, "VoltX Series," *Datasheet*, p. 2, 2023, [Online]. Available: https://www.madgetech.com/wp-content/uploads/2023/01/voltx-series-ss-.pdf.

[22] G. Freiderich, Unpublished. Monterey Bay Aquarium Research Institute.

[23] ATMEL, "SAM D21 SMART ARM-Based Microcontroller," *Datasheet*, p. 1111, 2015, [Online]. Available: https://cdn.sparkfun.com/datasheets/Dev/Arduino/Boards/Atmel-42181-SAM-D21_Datasheet.pdf.

[24] Maxim Integrated, "Extremely Accurate I 2 C-Integrated RTC DS3231," *Datasheet*, p. 19, 2015, [Online]. Available: http://datasheets.maximintegrated.com/en/ds/DS3231.pdf.

[25] Texas Instruments, "Ultra-Small, Low-Power, 12-Bit Analog-to-Digital Converter with Internal Reference," *Datasheet*, p. 33, 2009, [Online]. Available: https://cdn-shop.adafruit.com/datasheets/ads1015.pdf.

[26] Texas Instruments, "Ultra-Small, Low-Power, 16-Bit Analog-to-Digital Converter with Internal Reference," *Datasheet*, p. 36, 2009, [Online]. Available: http://www.ti.com/lit/ds/symlink/ads1115.pdf.

[27] Honeywell, "Durafet® Non-Glass pH Electrodes," *Datasheet*, p. 6, 2004, [Online]. Available: https://prod-edam.honeywell.com/content/dam/honeywell-edam/pmt/hps/products/pmc/process-instruments/analytical-instruments&sensors/ph-orp-sensors/durafet-ph-sensor/pmt-hps-70-82-03-50.pdf.

[28] Honeywell, "Durafet Cap Adapter," *Datasheet*, p. 2, 2010, [Online]. Available: https://prod-edam.honeywell.com/content/dam/honeywell-edam/pmt/hps/products/pmc/process-instruments/analytical-instruments&sensors/ph-orp-sensors/7777dvp-immersion-in-line-mounting/pmt-hps-70-82-03-66.pdf.

[29] B. V. Nemzer and A. G. Dickson, "The stability and reproducibility of Tris buffers in synthetic seawater," *Mar. Chem.*, vol. 96, no. 3–4, pp. 237–242, 2005, doi: 10.1016/j.marchem.2005.01.004.

[30] A. G. Dickson, "The measurement of sea water pH," *Mar. Chem.*, vol. 44, no. 2–4, pp. 131–142, 1993, doi: 10.1016/0304-4203(93)90198-W.

[31] E. Casilari, J. M. Cano-García, and G. Campos-Garrido, "Modeling of current consumption in 802.15.4/ZigBee sensor motes," *Sensors*, vol. 10, no. 6, pp. 5443–5468, 2010, doi: 10.3390/s100605443.

[32] A. Di Nisio, T. Di Noia, C. G. C. Carducci, and M. Spadavecchia, "High dynamic range power consumption measurement in microcontroller-based applications," *IEEE Trans. Instrum. Meas.*, vol. 65, no. 9, pp. 1968–1976, 2016, doi: 10.1109/TIM.2016.2549818.

[33] Keithley Instruments, "Model DMM6500 6½ Digit Bench/System Multimeter Specifications," *Datasheet*, p. 14, 2018, [Online]. Available: https://download.tek.com/document/SPEC-DMM6500A_April_2018.pdf.

[34] Rigol, "DS1000Z Series Digital Oscilloscope," *Datasheet*, p. 12, 2020, [Online]. Available: http://beyondmeasure.rigoltech.com/acton/attachment/1579/f-0317/1/-/-/-/-/DS1000Z Data Sheet.pdf.

[35] Onset, "HOBO® TidbiT® MX Temp 400 (MX2203) and Temp 5000

(MX2204) Logger Manual," *Datasheet*, p. 9, 2022, [Online]. Available: https://www.onsetcomp.com/resources/documentation/21537-mx2203-and-mx2204-manual.

[36] P. J. Bresnahan, T. R. Martz, Y. Takeshita, K. S. Johnson, and M. LaShomb, "Best practices for autonomous measurement of seawater pH with the Honeywell Durafet," *Methods Oceanogr.*, vol. 9, no. October, pp. 44–60, 2014, doi: 10.1016/j.mio.2014.08.003.

[37] P. J. Bresnahan *et al.*, "Autonomous in situ calibration of ion-sensitive field effect transistor pH sensors," *Limnol. Oceanogr. Methods*, vol. 19, no. 2, pp. 132–144, 2021, doi: 10.1002/lom3.10410.

[38] J. A. Newton, R. A. Feely, E. B. Jewett, P. Williamson, and J. Mathis, "Global Ocean Acidification Observing Network: requirements and governance Plan," *Glob. Ocean Acidif. Obs. Netw.*, no. October, pp. 5–28, 2015, [Online]. Available: www.iaea.org/ocean-acidification.

[39] A. Dementyev, S. Hodges, S. Taylor, and J. Smith, "Power consumption analysis of Bluetooth Low Energy, ZigBee and ANT sensor nodes in a cyclic sleep scenario," *2013 IEEE Int. Wirel. Symp. IWS 2013*, pp. 7–10, 2013, doi: 10.1109/IEEE-IWS.2013.6616827.

[40] A. Caviezel *et al.*, "Design and Evaluation of a Low-Power Sensor Device for Induced Rockfall Experiments," *IEEE Trans. Instrum. Meas.*, vol. 67, no. 4, pp. 767–779, 2018, doi: 10.1109/TIM.2017.2770799.

[41] L. J. Bradley and N. G. Wright, "Optimising SD Saving Events to Maximise Battery Lifetime for Arduino™/Atmega328P Data Loggers," *IEEE Access*, vol. 8, pp. 214832–214841, 2020, doi: 10.1109/ACCESS.2020.3041373.